Powder Technology 433 (2024) 119282

Contents lists available at ScienceDirect

Powder Technology

journal homepage: www.journals.elsevier.com/powder-technology

Optimisation of the performance of a new vertical roller mill by computational fluid dynamics simulations

Muzammil Ali [1], Alejandro López [2], Mehrdad Pasha [3], Mojtaba Ghadiri [*]

School of Chemical and Process Engineering, University of Leeds, Leeds, UK

HIGHLIGHTS

- The performance of a vertical roller mill is analysed with CFD.
- Adverse air circulation is detected through CFD simulations.
- Design modifications were evaluated and implemented.
- The detected issues were resolved, improving the performance.
- The erosion pattern inside the mill was calculated with CFD.

GRAPHICAL ABSTRACT

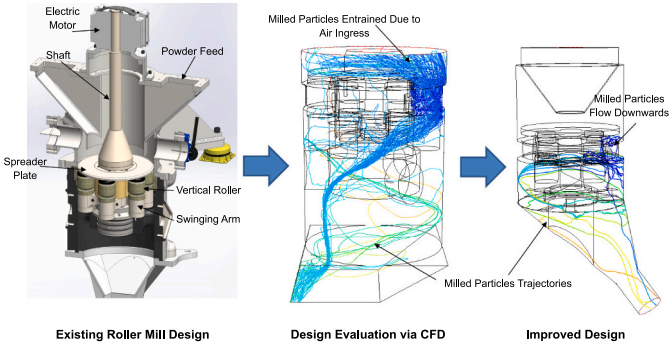

ARTICLE INFO

Keywords:
CFD
Milling
Vertical roller mill
Erosion

ABSTRACT

The performance of two new Vertical Roller Mills (VRM) has been analysed using Computational Fluid Dynamics (CFD). The results show notable air ingress from the bottom of the mill, due to moving components in the mill. This is detrimental to mill performance as the milled powder gets recirculated back into the milling region and reduces the overall milling efficiency. Optimisation of the mill design has been carried out based on CFD modelling results. Proposed reconfigurations produce a positive pressure upstream, suppressing air ingress. Design modifications were implemented in a pilot-scale mill, resolving the air ingress problem. Additionally, erosion patterns were computed for the mill geometry and qualitatively confirmed by visual inspection of the mill.

1. Introduction

Particle size distribution is one of the most important characteristics of powders for any industry involved in the production and/or handling of powders. Milling operation is carried out to reduce the particle size of raw materials for further processing and for finished products. Milling is very demanding in terms of energy consumption, accounting sometimes for the highest demand in the processing plant [1]. Roller mills are used

* Corresponding author.
E-mail address: m.ghadiri@leeds.ac.uk (M. Ghadiri).
[1] Fluid Comp Limited, Bradford, UK.
[2] Faculty of Engineering, University of Deusto, Spain.
[3] The Janssen Pharmaceutical Companies of Johnson & Johnson, Belgium.

https://doi.org/10.1016/j.powtec.2023.119282
Received 9 October 2023; Received in revised form 4 December 2023; Accepted 11 December 2023
Available online 14 December 2023

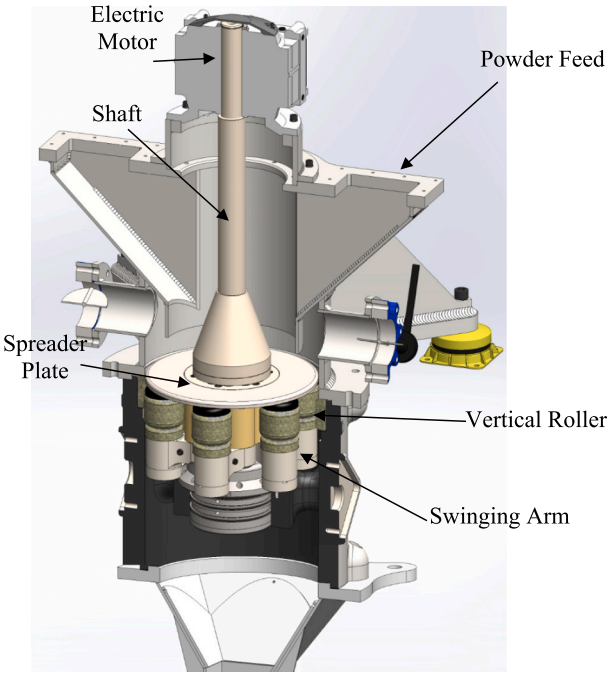

Fig. 1. M600 vertical roller mill by Hosokawa Micron.

increasingly for milling solids in a variety of industries including cement, power, chemicals, and mining. Particularly in the cement industry, ball mills have largely been replaced by roller mills for new plants [2], as they are compact, and the installation cost is smaller [3]. The vertical roller mills are up to 40% more energy efficient than ball mills [4]. The milled particles are typically a few microns to 100 μm in size. In traditional roller mills, the particles form a bed on a horizontal platen, and are crushed under rollers [5,6].

A number of single phase and multiphase Computational Fluid Dynamics (CFD) modelling studies have been carried out to study air flow profiles and particle trajectories in roller mills to optimise the performance and milling efficiency. Vuthaluru et al. [7] carried out multiphase CFD modelling of a roller mill to investigate air flow profiles and particle trajectories of different particle sizes. Vuthaluru et al. [8] carried out multiphase CFD modelling of a roller mill used as coal pulveriser to investigate wear pattern in the mill. Based on CFD modelling results, design changes were made to the inlet section to reduce the wear pattern. Sun et al. [9] carried out study of a roller mill (HRM 4800 by Hefei Zhong Ya, China) and analysed air flow patterns in the mill to improve the energy efficiency of the mill. Shah et al. [10] used modelling to optimise the performance of a coal pulveriser by studying the influence of variation in inlet vane angles on the collection efficiency of the powder and desired cut size. Ze et al. [11] modelled HRM 4800 mill to analyse the air and particles flow to determine optimised operating conditions for improved milling efficiency. Bhambare et al. [12] carried out multiphase CFD modelling of an MPS roller mill, considering drying of coal particles in the mill. By analysing the CFD modelling results, it was found that a non-uniform air distribution at the inlet section was mainly responsible for non-uniformity in the flow of particles at the outlet.

A recurrent issue in this type of mills is the high degree of erosion in the mill by the grinding ring as well as the rollers. A number of different empirical, numerical and analytical approaches have been used to predict erosion in the literature. Meng and Ludema [13] carried out a literature review including more than 5000 papers dating from 1957 to 1992. In their work, they encountered more than 2000 different equations for calculating erosion. Erosion is influenced by different variables

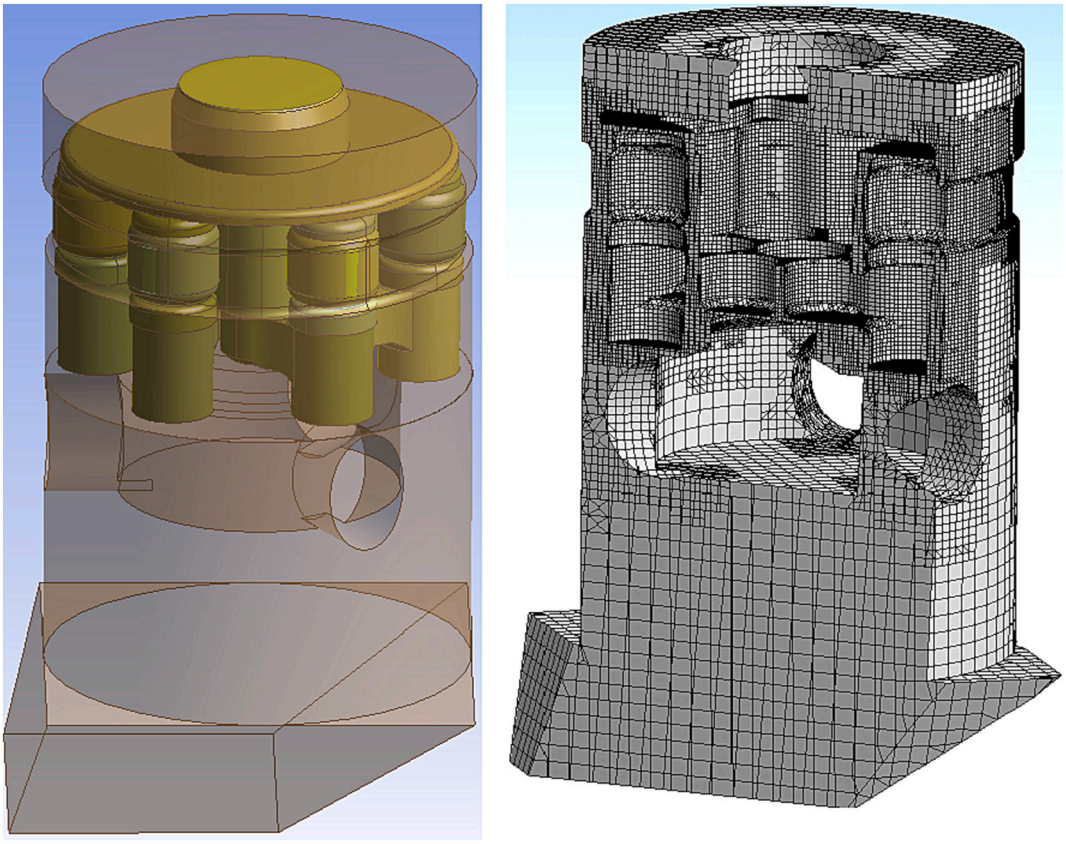

Fig. 2. M600 mill geometry and mesh considered for CFD modelling.

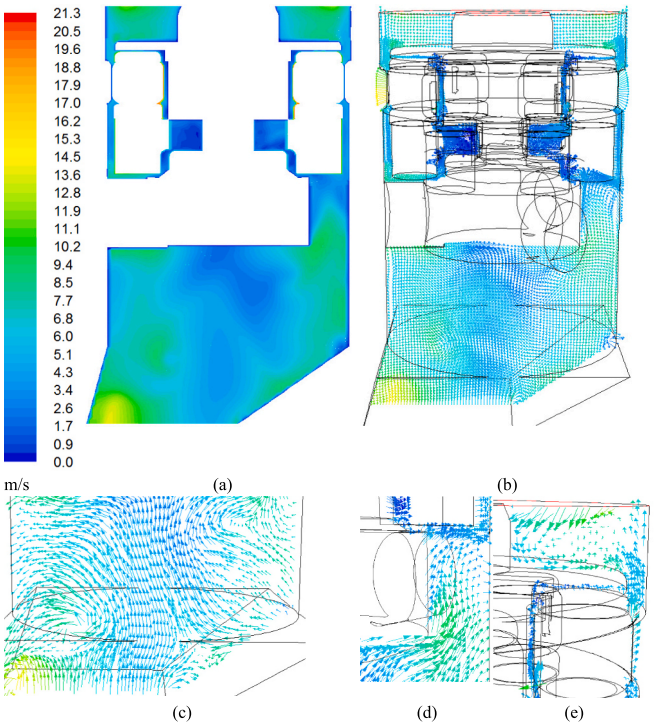

Fig. 3. CFD predicted results of M600. (a): Velocity magnitude contours; (b): Velocity vectors coloured by magnitude; (c): Close-up of the bottom of the mill with the velocity vectors coloured by magnitude showing upward flow; (d): Close-up of one of the rollers with velocity vectors coloured by magnitude showing recirculation; (e): Air flow above the spreader plate.

depending on the fluid flow properties and its pattern, material properties and properties of the abrasive particles. Humphrey [14] showed more than 20 factors affecting solid particle erosion which have been considered in the literature and grouped under three different categories. These three categories corresponded to the particle variables, the surfaces involved in the erosion process and the carrier fluid.

This study is concerned with evaluating the performance of a novel roller mill, in which the crushing platen is a vertical wall over which cylindrical rollers rotate, thereby crushing a raining bed of particles. It has been manufactured by International Innovation Technologies, Gateshead, UK. It has a small footprint, suitable for limited space. A particular feature of mills with internal rotating components is that the moving parts can induce air circulation, which may adversely affect the mill operation. Non-managed airflow presents several drawbacks, notably the potential for fine particles to become recirculated within the air stream, leading to their integration with coarser powders. This can result in diminished throughput and reduced milling efficiency due to the cushioning effect exerted by these fine particles, along with increased wear and tear. Consequently, it is imperative to conduct a comprehensive analysis of how the rotation of moving components within this mill impacts airflow, particle feeding, and accumulation.

The air flow inside the mill and its influence on the trajectories of milled particles are analysed using CFD approach. Design modifications are proposed and implemented in a pilot-scale mill to eliminate the adverse effects of air ingress and improve the mill performance. The erosion pattern inside the mill is also identified by analysing the fluid flow pattern likely to induce erosion.

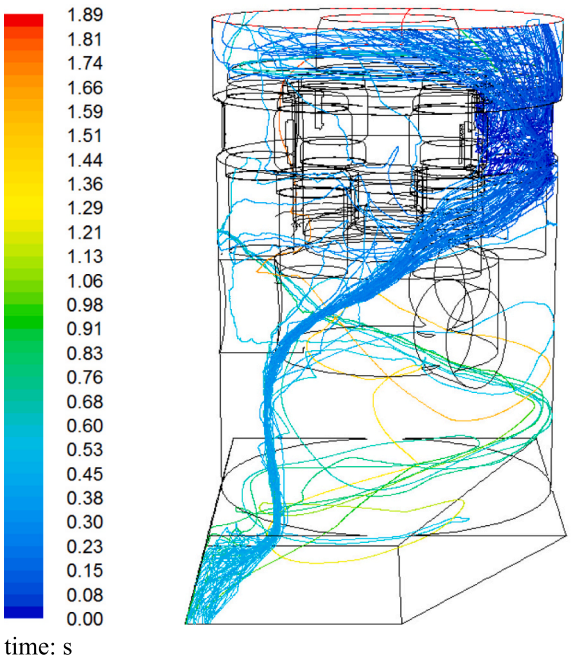

Fig. 4. Particle trajectories in M 600 mill coloured by residence time for 10 μm spheres (ρ = 800 kg/m^3).

2. Description of the vertical roller mill

An industrial-scale vertical roller mill (M600) was analysed for air flow in this study. This led to proposed modifications, which were implemented in a new mill design (M350). The M600 mill can operate under continuous mode and is used for fine grinding of materials. The design of this mill is depicted in Fig. 1. It comprises six vertical rollers mounted on swinging arms, which rotate on their own axis in addition to rotation by a central shaft. The latter is rotated at 450 RPM in a typical operation. The resulting centrifugal force presses the rollers against the wall. The feed is entered from the top using two feeding ports to the sides of the mill, introducing the particles to the spreader plate. The spreader plate rotates with the central shaft and spreads the particles towards the wear ring (vertical wall), where the particles get milled by the rotating rollers due to compressive forces. The milled powder rains down and exits from the bottom of the mill. The electric motor driving the mill is located above the feed inlet ports.

3. Modelling

To investigate air flow pattern in the mill and its influence on the particle trajectory, CFD modelling was carried out. The geometries were prepared and meshed with Design Modeller and Ansys Meshing by Ansys Workbench. The effect of the air flow induced by the rotating parts was analysed using the commercial CFD software Ansys Fluent to solve the governing equations. The turbulence was modelled using the Reynolds stress turbulence model, as this model gives a better prediction of fluid velocity profiles in flows involving swirling and rotating fluids compared to the eddy-viscosity based models. The second-order upwind scheme [15] was used for the discretisation of the convection terms. For the pressure-velocity coupling, the SIMPLE algorithm was used and for the pressure interpolation, Standard scheme [16] was used. For the air inlet and exit, the pressure boundary condition was specified at both the

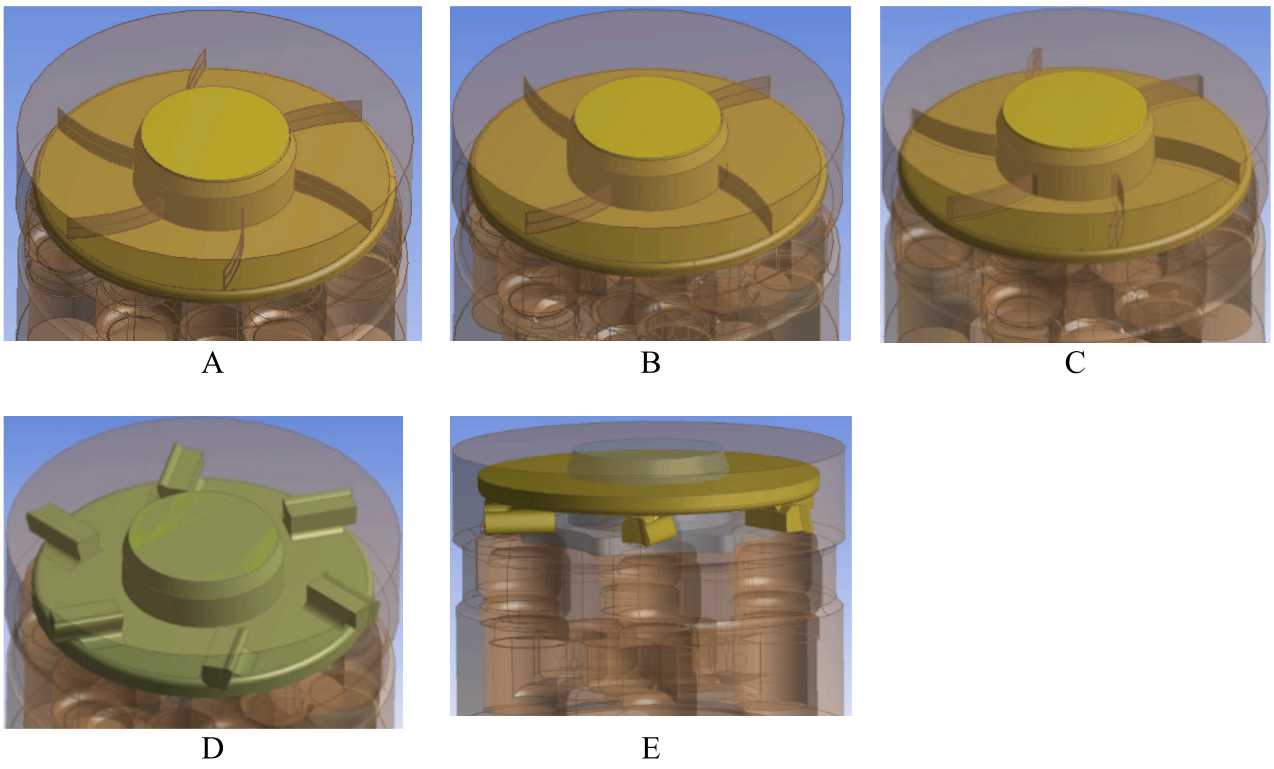

Fig. 5. Different vane designs on the spreader plate evaluated for eliminating air ingress.

Table 1
Air mass flow prediction for various spreader plate designs.

Design	A	B	C	D	E
Air ingress (kg/h)	+165	+24	+10	+5	−650

top face and the bottom face with zero gauge pressure (corresponding to atmospheric pressure). For the turbulence boundary conditions, hydraulic diameter and turbulence intensity with a value of 5% was specified. The modelling of flow near the wall is carried out using non-equilibrium wall functions with smooth wall (zero surface roughness) assumption. The air is considered to be incompressible as the density of the air is expected to be constant in this system. The central shaft rotates clockwise, and as the rollers are pressed against the wall, their rotation is anticlockwise. The central shaft rotation specification is 450 rpm (representing typical operation of the mill) and hence each roller rotation is considered to be 2022 rpm in the anticlockwise direction. The rotation of the central shaft and connected geometries is carried out using rotating reference frame method.

To ensure that the results produced by CFD modelling are mesh independent, a mesh independency test was carried out considering a series of different mesh sizes. The velocity profiles as well as the mass flow rate of air entrained were compared in all meshes. For a certain mesh size which was small enough to capture all relevant parameters, the changes in mass flow rate and velocity profiles became relatively small. If that size was decreased further, mass flow rate and velocity profiles remained virtually the same, ensuring that the previous mesh size was optimised for CFD calculations of the fluid parameters in the roller mill. Mesh sizes varied between 260,000 cells and 3 million cells. The selected mesh comprised 850,000 cells. The computation time for the selected mesh was 15 h for simulating 7 s of flow time on a 32 core 3.4 GHz processor CPU.

Convergence criteria were based on monitoring both the residuals as well as the difference between the inlet and outlet mass flow rates, making sure that these did not change appreciably with time before stopping the simulations. The geometry of the mill and the selected mesh are depicted in Fig. 2.

3.1. Air flow inside M600 mill

Fig. 3 (a) is a plot of contours of CFD predicted air velocity resulting from the rotation of the spreader plate, the roller arms and the connected vertical rollers. These plots are coloured by velocity magnitude along with arrows showing the direction of air flow in a vector plot in Fig. 3 (b). Fig. 3 (c) is a close-up view of velocity vector plot of air flow in the bottom region. Fig. 3 (d) is a vector plot of the region just below the roller arm. In Fig. 3 (e), the vector plot of air flow above the spreader plate is depicted. The air entrainment can clearly be observed from the bottom region of the mill, indicated by arrows in the upward direction, which can entrain the milled particles upwards as they pass through the rollers and rains downwards due to gravity. The air flow is in the upward direction near the walls around the spreader plate, which is undesirable as this can cause accumulation of feed at the spreader plate, particularly for relatively small size, low density powder, as well as entrainment of milled particles. Hence this design allows air ingress from the bottom of the mill as its arms and shaft rotate, which would entrain milled particles and reduce the milling efficiency. Total amount of entrained air is predicted to be 450 kg/h, which confirms the measurements of air flow taken from the mill. It should be noted that in the simulation, the powder flow is not considered. This would also have an impact on the air flow as the flow of powder in the mill is expected to have a dense loading particularly above the spreader plate and around the rollers.

3.2. Prediction of fine particle trajectories

The trajectories of fine particles are expected to be influenced by the surrounding air flow within the mill. In order to predict particle trajectories, Eulerian-Lagrangian calculation approach is used as described by Lopez et al. [17,18]. This is done to obtain a qualitative

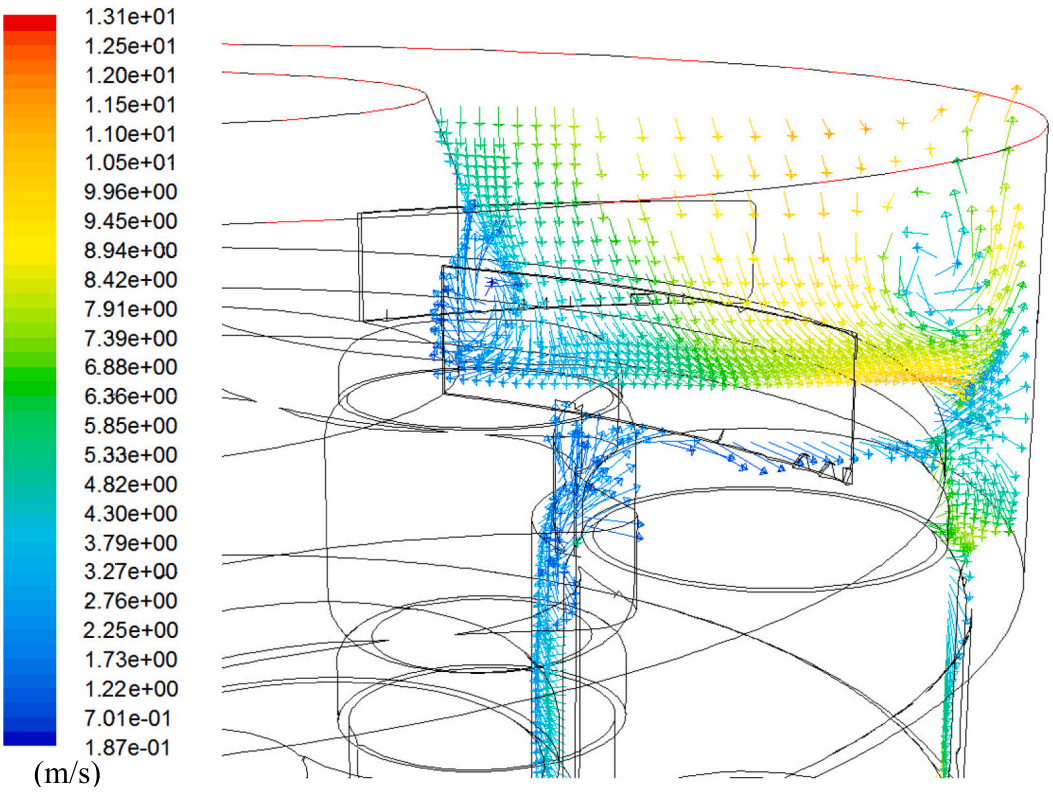

Fig. 6. Air flow patterns around the vanes at the top of the spreader plate coloured by velocity magnitude (m/s).

representation of the flow of milled particles below the rollers. The particles are considered to be mono-size, spherical and with a diameter of 10 μm, and an envelope density of 800 kg/m^3. The particles are injected from the surface of one of the rollers. One-way coupling is considered, i.e. the momentum exerted by the particles on the air and inter-particle interactions are ignored. The equations of motion of particles are solved considering the drag and gravitational forces. The drag law proposed by Morsi and Alexander [19] is used for the calculation of the drag coefficient. To consider the effect of turbulence on particle trajectories, the discrete random walk model [20] is used.

The trajectories of particles depicted in Fig. 4 are coloured by their residence time. Only about 20% of the particles by mass leave from the bottom while the remaining 80% get entrained. Hence the upward airflow is causing the majority of the milled particles to flow in the upward direction. Particles leaving from the top will get mixed with the coarse powder feed and eventually exit from the bottom or deposit on stationary surfaces, thus reducing the milling efficiency as the energy is being wasted in compression. Since milling takes place due to compressive force between the rollers and the wall, the presence of fine particles at the rollers reduces the indirect tensile stressing of particles during compression causing a cushioning effect, and hence more energy is required for milling.

3.3. Modified design evaluation

The CFD modelling results showed the necessity of design changes to eliminate the reverse air flow in the mill, as it is detrimental to the milling performance and efficiency. Hence, several design changes in the mill were evaluated using CFD modelling to study their influence on the air flow. Since the shaft and the connected geometry rotate, hence adding vanes in a direction that causes a fan effect can push the air downward. This was an option which was explored to eliminate this air ingress. A number of designs utilizing vanes on the spreader plate were evaluated. The modified spreader plate designs with vanes are depicted in Fig. 5.

In designs A and B, the height and thickness of the vanes are 40 mm and 2 mm, respectively. In design C, the thickness is 10 mm, while the height is kept the same. In design D the thickness of the vanes is increased. In design E, the spreader plate depicted in design D is reversed, i.e. mounted on the underside of the spreader plate. The predicted air ingress obtained from CFD modelling of all of the above cases is given in Table 1. The negative sign indicates air flow in the upward direction, while the positive sign indicates air flow in the downward direction. Therefore, designs A-D produce a net desirable downward air flow, but to different extents. Design A produces the largest downward air flow. In design E, in which the vanes are on the lower surface of the spreader plate, the air flow is actually increased in the upward direction. It would have been advantageous to have vanes in the downward direction as this results in minimized wear of the vanes. In Fig. 6, the air flow pattern around the vanes for design A is depicted. Strong recirculating regions are observed in the top spreader plate. This can cause choking of feed particles, hence reduced throughput and increased wear rate.

Having the vanes rotating at high RPM and colliding with the particles is likely to cause increased wear of the vanes. Therefore, although adding vanes at the top of the spreader plate eliminates air ingress, this can potentially cause an increased wear rate. Therefore, alternate changes were explored in which the vanes do not come in direct contact with the feed particles. One such change was adding the vanes in the top region of the rotating shaft. The modified design is depicted in Fig. 7 (a). Contours of axial velocity profiles resulting from the above change in the design are depicted in Fig. 7 (b). Positive values indicate air flow in the upward direction. In the bottom outlet, a relatively high air velocity in the upward direction can be observed, which would entrain milled particles. The net air flow obtained from this modification was 240 kg/h in the upward direction. The overall air flow pattern below the rollers is

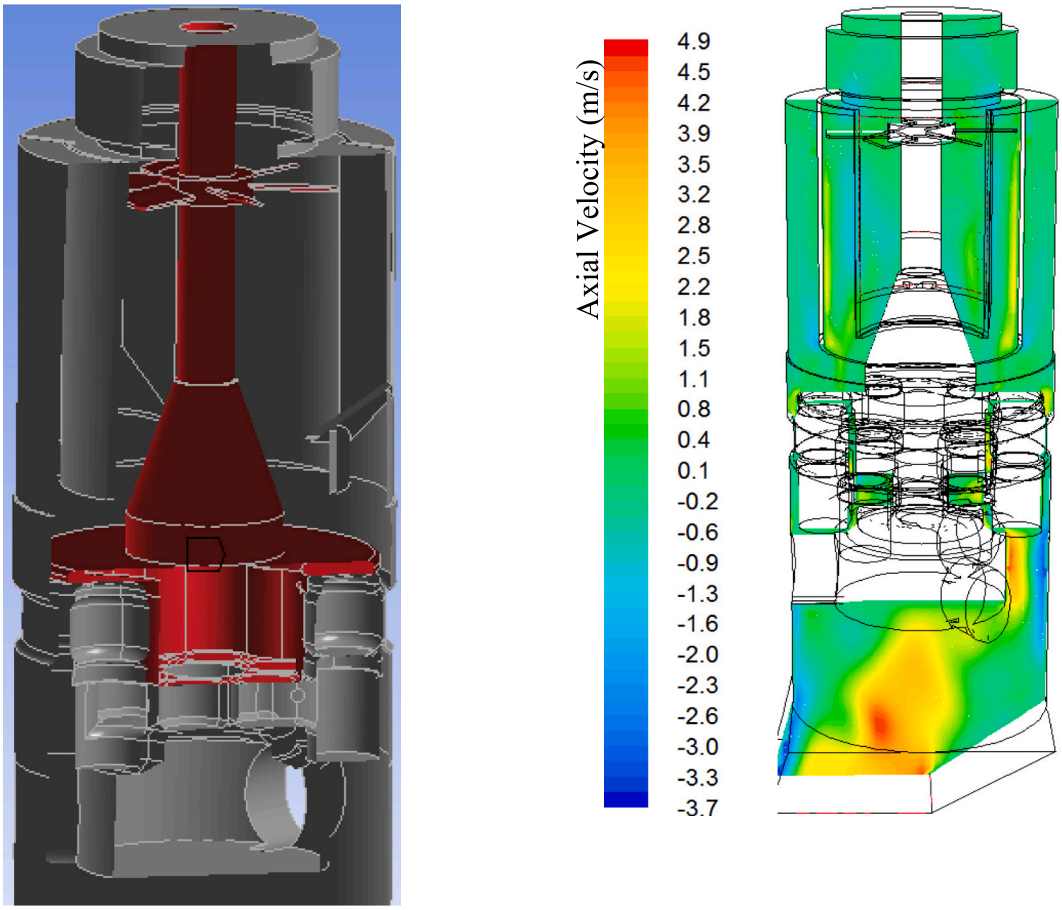

Fig. 7. M600 mill. (a): Modified geometry; (b): CFD predicted contours of air axial velocity profile.

similar to the air flow pattern predicted in the original design without any modification (Fig. 3 (a)). Hence the addition of vanes above the spreader plate does not result in net flow moving in the downward direction. This was attributed to the fact that the top section where the fan is located is enclosed which only results in local recirculation of the surrounding air. Hence, a further change was made and a number of openings were made in the top section, which are depicted in Fig. 8 (a) to allow the air to get entrained from the top.

Fig. 8 (b) is a vector plot of predicted air flow profile in the top shaft region, which is highlighted in red in Fig. 8 (a) showing a downward air flow. Hence the air is entrained from the top openings. However, the net air flow is still 144 kg/h in the upward direction as most of the air flow entrained from the top openings is exhausted from the feed particle inlet openings. Hence adding a fan at the top section of the mill does not result in appreciable reduction of air ingress from the bottom.

Design evaluation of the modified top feeding section of the mill (depicted in Fig. 9 (a)) was carried out. Since the particles are fed using a conical feeder close to the centre of the spreader plate, it is expected to cause a more uniform spread of particles on the wear ring. A cylindrical enclosure is added to prevent the particles from directly hitting the rotating shaft to prevent wear of the shaft.

Fig. 9 (b) is a vector plot of predicted air flow profile. No net air flow was found for this geometry. Hence this design eliminates air ingress without adversely affecting the wear rate. The throughput of the mill is also expected to be improved with this design, because the feed powder will get a more uniform spread on the platen in contrast to the existing design in which powder is fed from the sides and falls non-uniformly and closer to the edge of the spreader plate. Having a neutral flow would also allow more efficient milling of materials requiring an inert environment.

3.4. CFD modelling of M350 mill

The modified feeding section of the M600 mill was implemented in a pilot-scale mill (M350). This mill has four vertical rollers. The electric motor is placed below the spreader plate to avoid direct contact of the shaft with feed particles. The methodology used to predict the air flow in the M350 mill is the same as the one used for the M600 mill. Pressure outlet boundary condition at the top inlets and the bottom outlet was specified with a value of zero gauge pressure. The geometry considered for CFD modelling and the selected mesh (comprising 1.3×10^6 cells) are depicted in Figs. 10 (a) and (b), respectively.

The predicted vectors of air velocity coloured by magnitude of velocity components and the path lines of air flow in the mill are depicted in Figs. 11 (a) and (b). A jet of air impinges on the spreader plate from the conical feeder opening; this pushes the air in the downward direction. The air flow is also in the downward direction at the bottom outlet region. The net downward air flow is predicted to be 180 kg/h. Hence the design of the M350 mill is not expected to have undesirable retention and recirculation of fine particles. There is no net upward or downward flow of air in the industrial scale M600 mill after the addition of a cone feeder modification. In the M350 design, no cylindrical enclosure is required for the shaft in the top conical feeder, since the motor is located below the spreader plate.

To predict trajectories of the milled particles using CFD modelling,

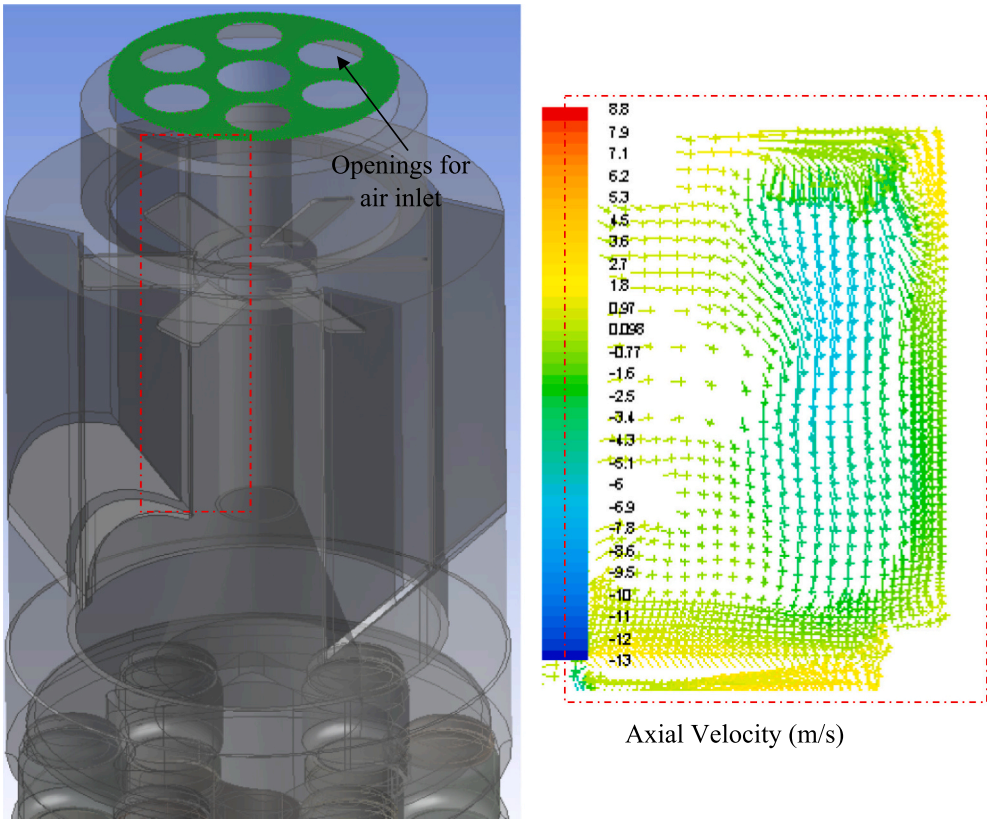

Fig. 8. M600 mill. (a): Modified geometry; (b): predicted axial velocity vectors.

particles having a diameter of 100 μm and a density of 1500 kg/m^3 are released from one of the surfaces of the rollers and tracked using the Eulerian-Lagrangian approach. The predicted particles trajectories are depicted in Fig. 12 and are coloured according to their residence times.

As opposed to the trajectories observed in M600 mill without the cone feeder design, all the particles have a net downward movement. Although some recirculation of particles is observed just below the rollers, but all the particles eventually exit from the bottom outlet. Hence the possibility of mixing of feed with milled particles is minimum in this mill. The existing M350 mill design is expected to perform better in terms of particles and air flow dynamics and would result in better milling efficiency compared to the existing design of M600 mill.

3.5. Assessment of the locations of maximum erosion

CFD simulations can be used to estimate erosion rates in different kinds of equipment. A very large number of papers have been published on the topic [21] and, as a result, there are many different equations and approaches used in its prediction. Different authors have adopted their own approach to erosion, based on the mechanisms they have deemed important. Two of the mechanisms for solid particle impingement that, at least a few authors agree on, are cutting and deformation wear. Cutting wear occurs at low angles of impingement and particles tear the material away as they hit the surface. Deformation wear is a result of repeated impacts at high angles of impingement, where the surface of the material is repeatedly hit and hardened when the kinetic energy is enough to induce plastic deformation. After a number of impacts, the material might reach a point, where small platelets detach after not being able to withstand any more plastic deformation. When dealing with rotating machinery, vorticity has proven to be a good estimator of the locations of erosion. In the case of centrifugal pumps, the relationship between vorticity and erosion rate has been investigated by Cai et al. [22]. The underlying consideration is that most of the erosion is induced by small particles, which impact due to vorticity. These particles have a small Stokes number, thereby following the fluid flow more closely, in contrast to large particles that have higher inertia and deviate from the fluid stream line. The plot of the vorticity magnitude at the surfaces of the rotating geometry can be used to find the locations of the maximum erosion. The erosion pattern can therefore be studied by analysing the magnitude of the fluid vorticity at the eroded walls.

The geometry analysed was the latest modification of the M350 mill, which included the latest spreader plate design, as depicted in Fig. 13. The wear pattern predicted by the CFD model is depicted in Figs. 14–16. The areas identified as being subjected to a higher erosion rate are the surfaces of the roller, ring, spreader plate (especially at the sharper edges) and the areas surrounding the rollers. These areas correspond to regions where the fluid exhibits abrupt changes, usually induced by sharp geometrical configurations, sudden changes in sections or curvature and areas with high velocity gradients. In the case of Figs. 15 and 16, the areas with the highest erosion rate also coincide with the geometry parts subjected to the highest tangential velocities, while in Fig. 14, the most significant erosion is expected in the area where the rollers meet the side walls of the geometry. In this area however, more erosion is also expected due to the friction between the rollers and the material being constantly crushed against the walls of the mill. Visual inspection of the M350 mill indicated similar wear pattern generated in the CFD simulations, thus giving qualitative validation of the approach [23]. This also supports the consideration that the smaller particles are responsible for most of the erosion. However, more experimental tests would be necessary for a quantitative validation.

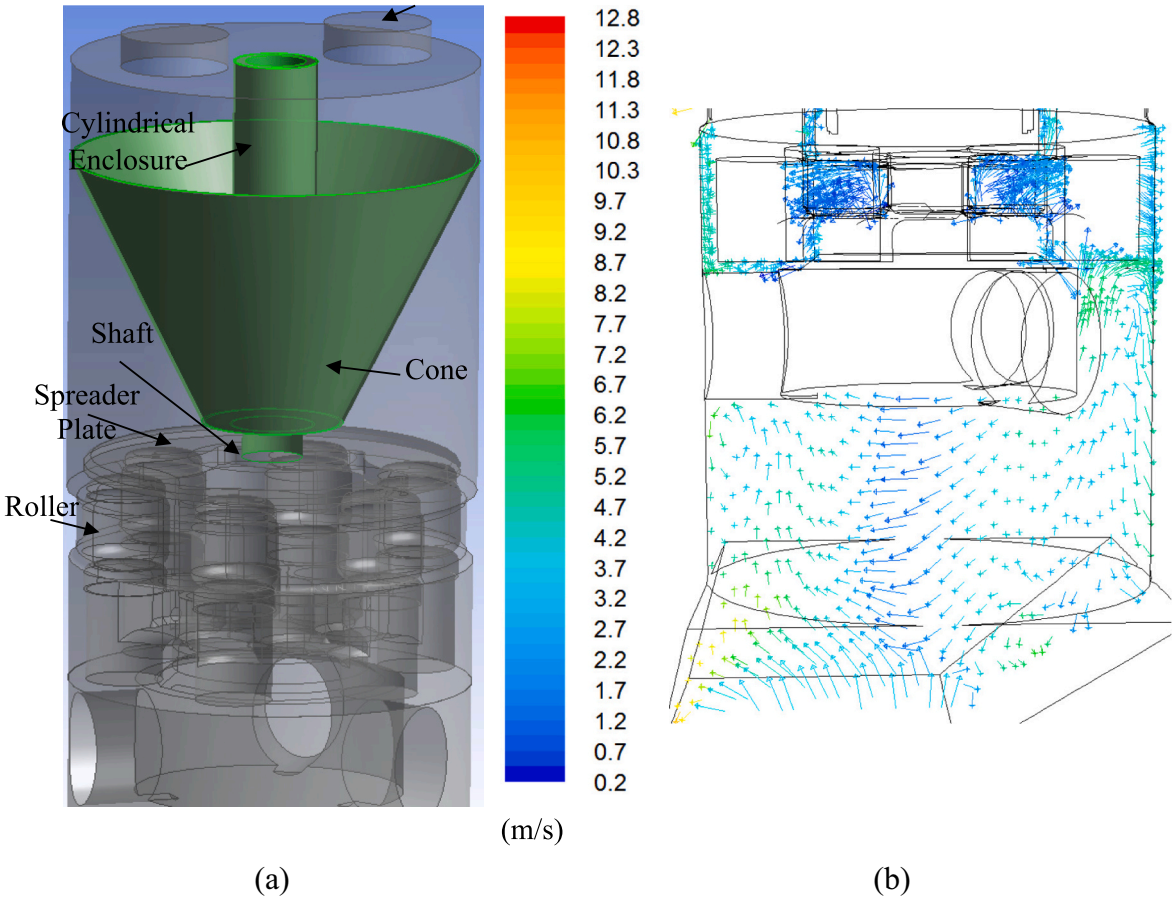

Fig. 9. M600 with modified powder feeding section. (a): Modified geometry; (b): Predicted air velocity vector plot.

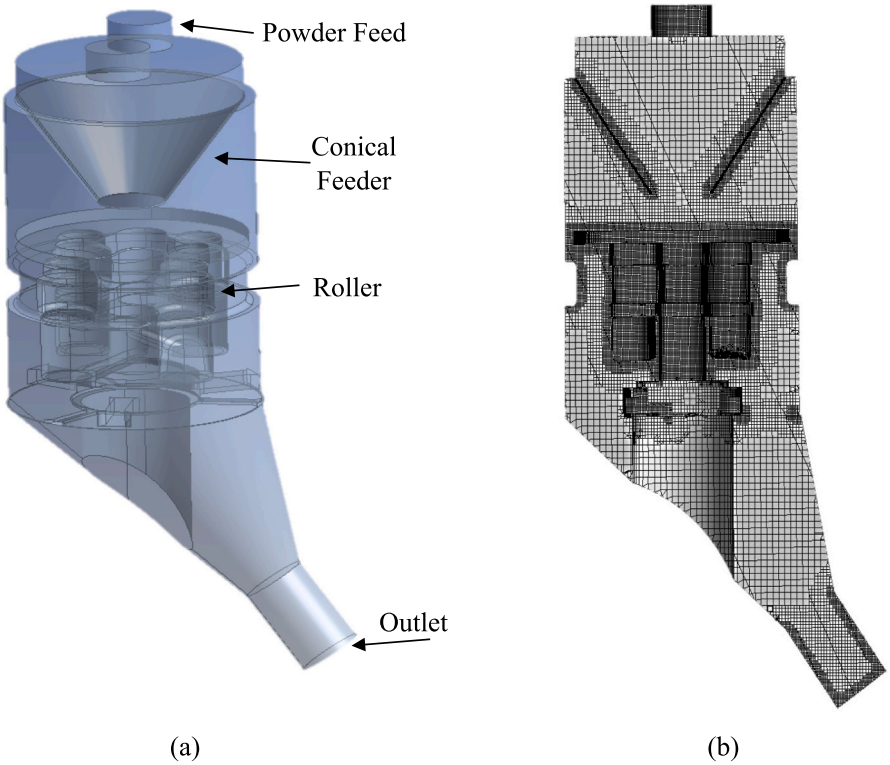

Fig. 10. M350 mill. (a): Geometry; (b): Mesh used in CFD modelling.

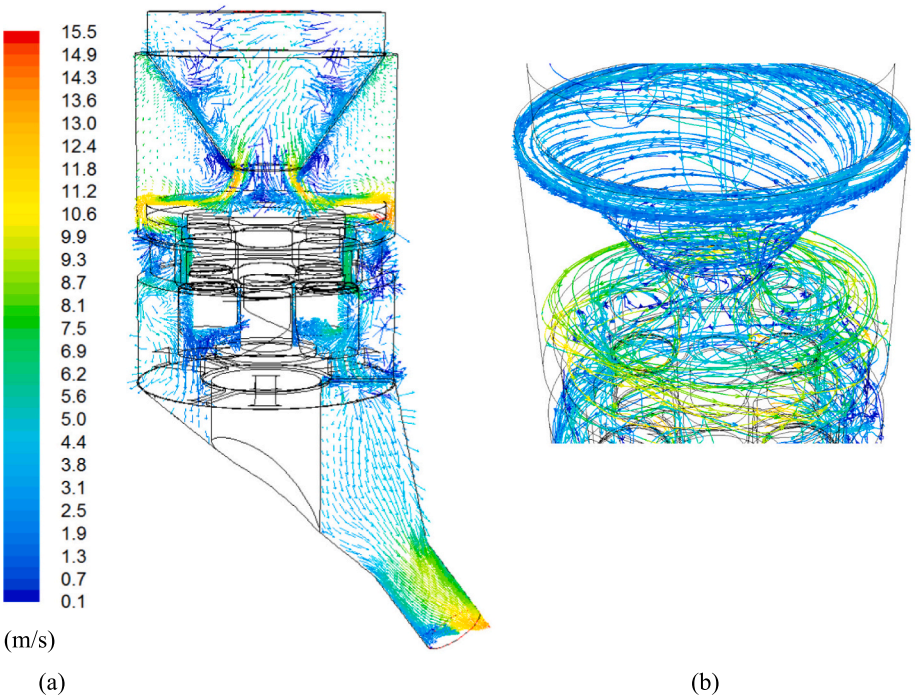

Fig. 11. M350 mill. (a): Air velocity vectors; (b): Air flow path lines.

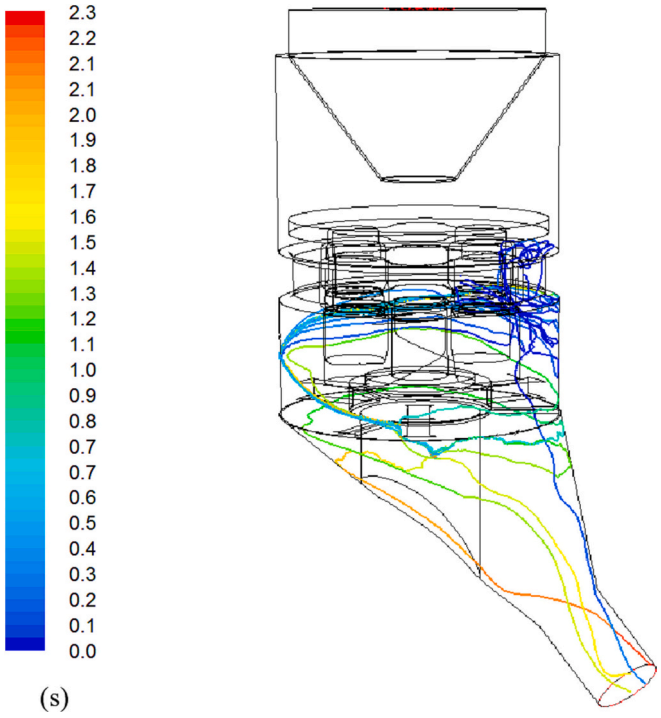

Fig. 12. Predicted trajectories of particles in M350 mill coloured by residence times.

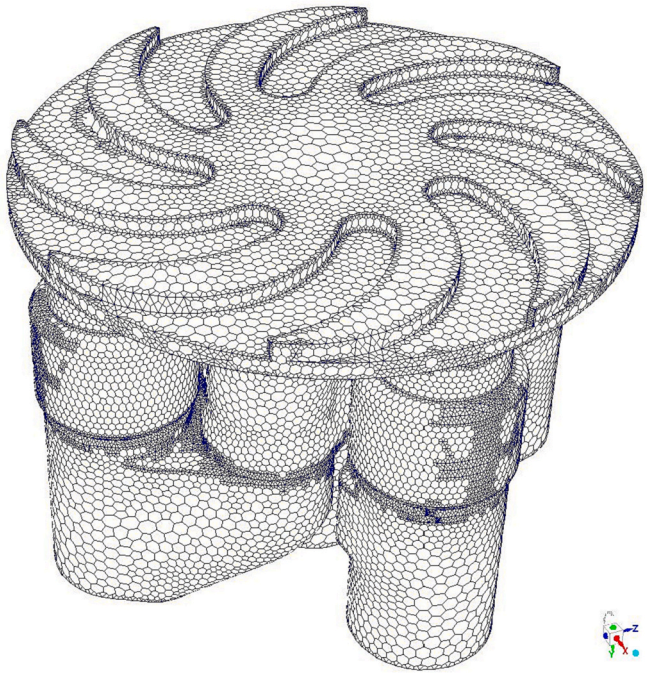

Fig. 13. Spreader plate final design.

4. Conclusions

CFD modelling has been carried out to analyse and optimise the design and operation of the Vertical Roller Mill. CFD model is coupled with Lagrangian approach to assess the influence of air flow on the trajectory of milled particles. The results showed air ingress from the bottom outlet in the industrial-scale mill (M600), which was found to be detrimental to its performance. Several design changes and their influence on air flow profiles were explored using CFD to counteract the reverse air flow. It was found that adding a top cone feeding system would eliminate the reverse air flow in the mill and it would also result in more uniform distribution of feed on the spreader plate, which would result in higher milling efficiency and allow it to run at higher capacity. Analysis of air flow in a pilot-scale vertical roller mill (M350) were also carried out. The new design of the mill due to the presence of cone feeder prevented any air ingress from the bottom of the mill, a highly desirable

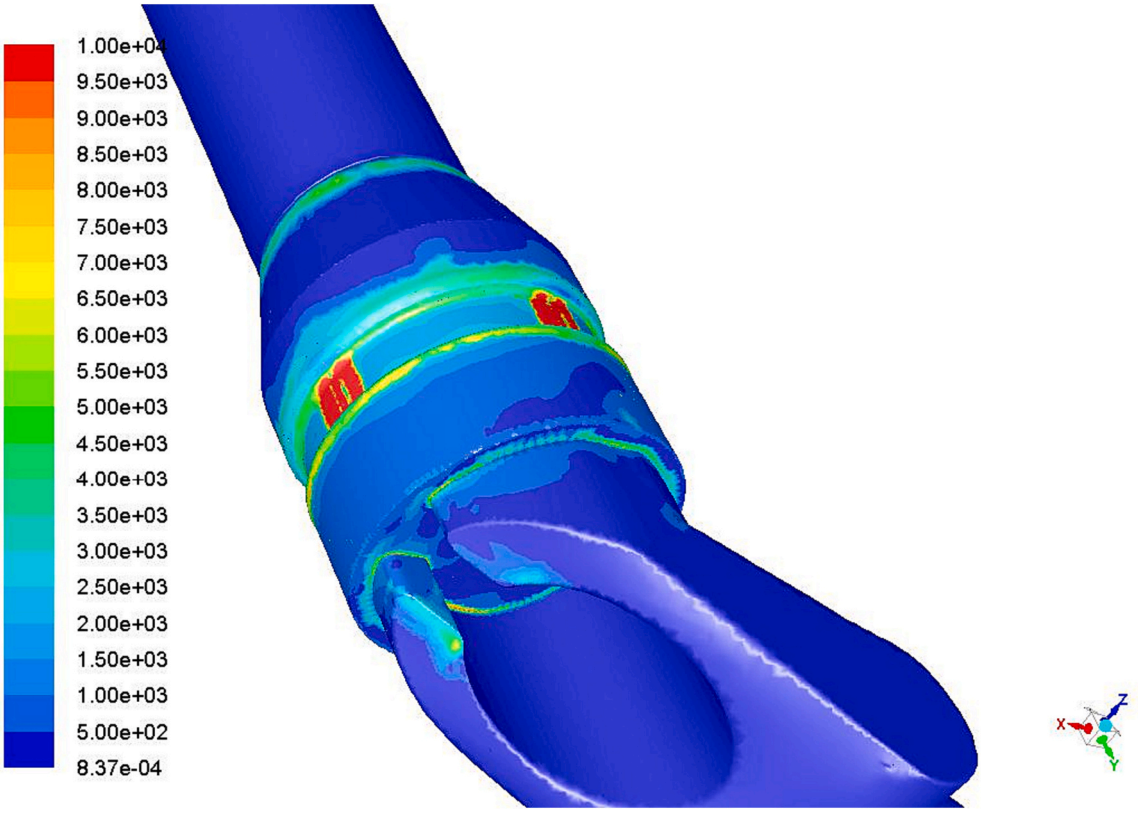

Fig. 14. Location of areas of fluid pattern inducing erosion on the ring and VRM lower walls.

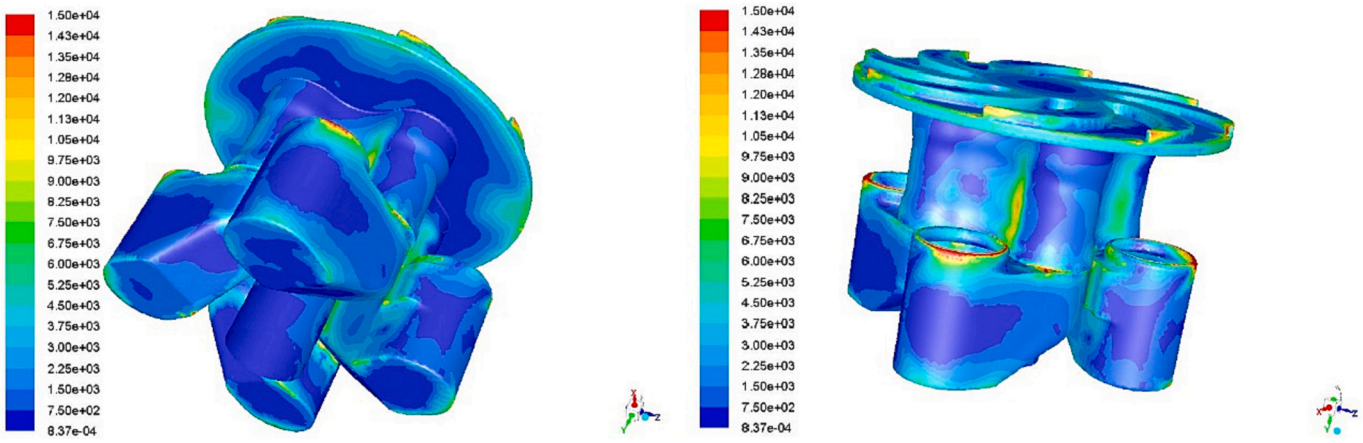

Fig. 15. Location of areas of fluid pattern inducing erosion on rotating components.

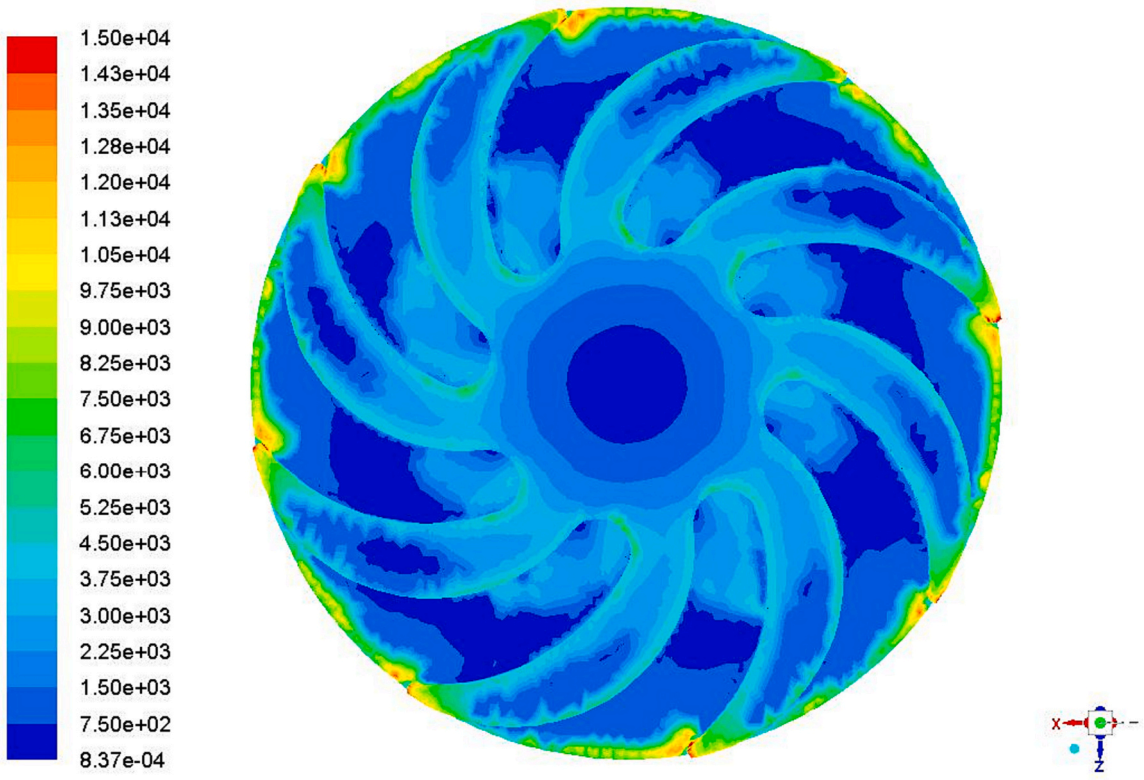

Fig. 16. Location of areas of fluid pattern inducing erosion on the spreader plate.

outcome. Erosion patterns were predicted for the whole geometry by analysing the vorticity patterns which were validated qualitatively by visual inspection of M350 mill. An improved version of the mill geometry against erosion could be achieved by smoothening the sharp edges that exhibit the highest values of vorticity.

CRediT authorship contribution statement

Muzammil Ali: Investigation, Methodology, Software, Supervision, Validation, Visualization, Writing – original draft, Writing – review & editing. **Alejandro López:** Investigation, Methodology, Software, Visualization, Writing – original draft, Writing – review & editing. **Mehrdad Pasha:** Investigation, Methodology, Software, Visualization, Writing – original draft, Writing – review & editing. **Mojtaba Ghadiri:** Investigation, Supervision, Writing – original draft, Writing – review & editing, Conceptualization, Funding acquisition, Methodology, Project administration.

Declaration of Competing Interest

The authors declare that they have no known competing financial interests or personal relationships that could have appeared to influence the work reported in this paper.

Data availability

The data that has been used is confidential.

Acknowledgements

The financial support of The Advanced Manufacturing Supply Chain Initiative (AMSCI), UK, for funding this project through the Chariot Programme is gratefully acknowledged. The authors would like to thank Professor David York, the Principal Investigator of the Chariot Programme for his initiative, vision and support and Mr. Paul Gould, P&G, for his overall coordination of the project. The authors are also thankful to Ms. Clare Martin and Dr. Nigel-Sommerville-Roberts at Procter & Gamble Technical Centres Ltd., Newcastle upon Tyne UK, and Messrs. Richard Bond and Mr. Dan Larkman at International Innovative Technologies for useful discussions.

References

[1] D. Altun, H. Benzer, N. Aydogan, C. Gerold, Operational parameters affecting the vertical roller mill performance, Miner. Eng. 103-104 (2017) 67–71.
[2] J. Harder, Grinding trends in the cement industry, ZKG International, 2010 issue 4-2010.
[3] M. Mutter, Cement grinding – VRM or ball mill? World Cement, 2013 issue 3-2013.
[4] M. Simmons, L. Gorby, J. Terembula, Operational experience from the United States first roller mill for cement grinding, in: IEEE-IAS/PCA Cement Industry Conference, 15-19 May, 2005, USA, 2005.
[5] L.R.D. Jensen, Wear mechanism of abrasion resistant wear parts in raw material vertical roller mills, Wear 271 (2011) 2707–2719.
[6] H.U. Schaefer, Loesche vertical roller mills for the comminution of ores and minerals, Miner. Eng. 14 (2001) 1155–1160.
[7] H.B. Vuthaluru, V.K. Pareek, R. Vuthaluru, Multiphase flow simulation of a simplified coal pulveriser, Fuel Process. Technol. 86 (2005) 1195–1205.
[8] R. Vuthaluru, O. Kruger, M. Abhishek, V.K. Pareek, H.B. Vuthaluru, Investigation of wear in a complex coal pulveriser using CFD modelling, Fuel Process. Technol. 87 (2006) 687–694.
[9] Y. Sun, X. Ze, X. Yang, C. Zhang, Yiqi Zhou, Analysis of flow field in vertical roller mill chamber based on turbulent models, in: International Conference on Environmental Science and Information Application Technology, 4-5th July, 2009, China, 2009.
[10] K.V. Shah, R. Vuthaluru, H.B. Vuthaluru, CFD based investigations into optimization of coal pulveriser performance: effect of classifier vane settings, Fuel Process. Technol. 90 (2009) 1135–1141.
[11] X.B. Ze, Y.W. Sun, W. Wang, J.L. Nie, K. Mao, Analysis of gas-solid coupling flow field in a vertical roller mill under different gas fluxes, J. Process Mech. Eng. 225 (2010) 20–28.
[12] K.S. Bhambare, Z. Ma, P. Lu, CFD modelling of MPS coal mill with moisture evaporation, Fuel Process. Technol. 91 (2010) 566–571.
[13] H.C. Meng, K.C. Ludema, Wear models and predictive equations: their form and content, Wear 181 (1995) 443–457.
[14] J.A.C. Humphrey, Fundamentals of fluid motion in erosion by solid particle impact, Int. J. Heat Fluid Flow 11 (1990) 170–195.

[15] S.V. Patankar, Numerical Heat Transfer and Fluid Flow, Hemisphere, Washington, 1980.
[16] H.K. Versteeg, W. Malalasekera, An Introduction to Computational Fluid Dynamics, Longman, Harlow, 2007.
[17] A. Lopez, M. Stickland, W. Dempster, CFD study of jet impingement test erosion using Ansys fluent and OpenFOAM, Comput. Phys. Commun. 197 (2015) 88–95.
[18] A. Lopez, M. Stickland, W. Dempster, CFD study of fluid flow changes with erosion, Comput. Phys. Commun. 227 (2018) 27–41.
[19] S.A. Morsi, A.J. Alexander, An investigation of particle trajectories in two-phase flow systems, J. Fluid Mech. 55 (2) (1972) 193–208.
[20] P. Hutchinson, G.F. Hewitt, A.E. Dukler, Deposition of liquid or solid dispersions from turbulent gas streams: a stochastic model, Chem. Eng. Sci. 26 (1971) 419–439.
[21] H.C. Meng, K.C. Ludema, Wear models and predictive equations, their form and content, Wear 181–183 (2023) 443–457.
[22] X. Cai, S. Zhou, Li., S., Study on the influence of back blade shape on the wear characteristics of centrifugal slurry pump, IOP Conf. Ser. Mater. Sci. Eng. 129 (2016) 12–58.
[23] R. Bond, Personal Communication at International Innovative Technologies, Gateshead, UK, 2016.